Talanta 83 (2011) 1754–1762

Contents lists available at ScienceDirect

Talanta

journal homepage: www.elsevier.com/locate/talanta

Overall calibration procedure via a statistically based matrix-comprehensive approach in the stir bar sorptive extraction–thermal desorption–gas chromatography–mass spectrometry analysis of pesticide residues in fruit-based soft drinks

Irma Lavagnini, Alessandro Urbani, Franco Magno*

Department of Chemical Sciences, University of Padova, Via Marzolo 1, 35131 Padova, Italy

ARTICLE INFO

Article history:
Received 27 May 2010
Received in revised form
19 November 2010
Accepted 5 December 2010
Available online 13 December 2010

Keywords:
SBSE–TD/GC–MS
Isotopically labelled/unlabelled internal standard
Pesticide residues
Fruit-based soft drinks
Variance component model

ABSTRACT

Stir bar sorptive extraction (SBSE)–thermal desorption (TD) procedure combined with gas chromatography mass spectrometry (GC–MS) and the statistical variance component model (VCM) is applied to the determination of semi-volatile compounds including organochlorine and organophosphorus pesticides in various synthetic and real fruit-based soft drink matrices. When the matrix effects are corrected using isotopically labelled or non labelled internal standard, but matrix/calibration run-induced deviations are still present in the measurements, the adoption of a variance component model (VCM) in the quantitative analysis of various matrices via an overall calibration curve is successful. The method produces an overall calibration straight line for any analyte accounting for the uncertainty due to all the sources of uncertainty, namely matrix-induced deviations, calibration runs performed at different times, measurement errors. Small increases in the detection limits and in uncertainty in the concentration values obtained in the inverse regression face favourably the decrease in times and costs for routine analyses.

1. Introduction

In recent years stir bar sorptive extraction (SBSE) [1,2] has found successful application in the analysis of drink contaminants [3–5] even if quantification can result sometime quite troublesome.

The main advantages are high recoveries and a concentration capability, due to the high volume of polymeric coating, and a solventless character, that makes it an environmentally friendly sample preparation technique [3]. A heavy drawback can be a significant matrix effect influencing the partitioning equilibrium and the recovery. Different methods can be used to compensate for the matrix effects, namely preparation of calibration solutions with a blank matrix matching closely the real matrix, addition of isotopically labelled internal standard (IS) and standard addition of the target solutes.

When isotopically labelled internal standards are not available, situation very frequent with a high number of analytes, the use of a non isotopically labelled IS does not completely compensate the matrix effect leaving a residual matrix-induced deviation. This problem is particularly important when the analysis of the same analyte is to be done in several matrices. Furthermore in routine analysis elapsing for a long period time-induced deviations can rise, requiring frequent time consuming calibrations. Recently in the GC–MS analyses of the target analytes in a wide range of matrices, for instance of veterinary [6] and human [7] medicine interest, and wine [8], the addition of variability coming from matrix- and calibration run-induced deviations has been treated using a statistically based approach called variance component model (VCM). This procedure represents an application of the random model ANOVA procedure [9] to the calibration straight lines obtained in different matrices and different times (both random factors) replacing them with a single comprehensive one of straightforward application. In this way apart from the IS used, the possible residual variability present in the data coming from the analyses performed in different matrices and/or in different times is properly accounted for.

The VCM procedure offers flexibility and a greater perspective than the conventional and far spread weighted least-squares regression [10] in which analyte measurements at different concentration levels in different matrices are considered as data sets of non-constant variance.

Since the analysis of pesticide residues in fruit-based soft drinks is at present time of the up most importance for their quite high level in highly consumed products [11,12], we studied the performance of coupling SBSE, recovery through thermo-desorption

* Corresponding author.
E-mail address: franco.magno@unipd.it (F. Magno).

0039-9140/$ – see front matter © 2010 Elsevier B.V. All rights reserved.
doi:10.1016/j.talanta.2010.12.004

Table 1
Matrix solutions used.

	Synthetic matrices			
	Matr.1	Matr.2	Matr.3	Matr.4
Saccharose	120 g/L	120 g/L	120 g/L	120 g/L
Citric acid	3 g/L	3 g/L	3 g/L	3 g/L
Pectin	–	2 g/L	10 g/L	4 g/L

	Fruit-based soft drink real matrices			
	Matr.A	Matr.B	Matr.C	Matr.D
	Lemon	Tropical juice	Orange	Mixed juice

Table 2
Mixtures used to obtain the extraction time profiles for any analyte.

Number of mixture	Matrices					
	Water	Matr.1	Matr.2	Matr.3	Matr.A	Methanol
1	5 mL	5 mL	–	–	–	–
2	5 mL	–	5 mL	–	–	–
3	5 mL	–	–	5 mL	–	–
4	5 mL	–	–	–	5 mL	–
5	4 mL	–	–	5 mL	–	1 mL
6	4 mL	–	–	–	5 mL	1 mL
7	10 mL	–	–	–	–	–
8	9 mL	–	–	–	–	1 mL
9	30 mL	–	–	–	5 mL	–

(TD), GC–MS analysis with the VCM statistical procedure to account for the contribute of uncertainty coming from matrix- and time-induced deviations. This question can be particularly important both as isotopically labelled ISs are commercially available for only few solutes and as the request of reducing the frequency of calibration is particularly considered in view of gaining the most cost-effective pesticide residue analysis.

The approach proposed in the present work is evaluated considering thirteen typical semi-volatile apolar compounds including chlorinated and organophosphorus pesticides, that, although banned, may be still present in fruit-based soft drink matrices, as proved in this study. The measurements were performed using both synthetic and commercially available matrices.

2. Experimental

2.1. Chemicals and reagents

Acetone standard solutions of ethyl parathion [56-38-2], methyl parathion [298-00-0], chlorpyriphos [2921-88-2], terbuphos [13071-79-9], fenthion [55-38-9] and chlorpyriphos methyl [2921-88-2] were purchased from Ultra scientific (Northkingstown, RI). Acetone standard solutions of endosulfan sulphate [1031-07-8], endrin [72-20-8], endrin ketone [53494-70-5], heptachlor [76-44-8], heptachlor epoxide [1024-57-3], lindane [58-89-9], and alachlor [15972-60-8] were purchased from Supelco (Oakville, Canada). Acetone solution of the internal standard d_{10}-chlorpyriphos

Table 3
Operating conditions for thermal desorption and GC run.

	Time interval				
	0–0.5 min	0.5–3.5 min	3.5–8.5 min	8.5–9.0 min	9.0–49 min
Temperature of thermal-desorption unit (°C)	80[a]	80–300[b] (70 °C min^{-1})[c]	300	300	300–80
Temperature of thermal-desorption unit transfer (°C)	300	300	300	300	300
Temperature of cooled injection system (°C)	20[a]	20[a]	20[a]	20–300[b] (10 °C s^{-1})[c]	300[d]
Temperature of column oven (°C)	75	75	75	75	75–100 (30 °C min^{-1})[c] 100–280 (5 °C min^{-1})[c]
Helium flux (mL min^{-1})	50	50	50	24.2	24.2
Pressure (psi)	9	9	9	9	9–26.8

[a] Solvent mode.
[b] Splitless mode.
[c] Temperature gradient.
[d] Splitless mode for 0.5 min and then split mode.

Table 4
Retention time (RT) and ion used in the quantitation and confirmation of analytes.

Analyte	RT (min)	Quantitation ion (m/z)	Qualifier ions (m/z)
Terbuphos	19.55	231	57, 10
Lindane	19.95	181	183, 219
Chlorpyriphos methyl	21.95	286	288, 125
Alachlor	22.14	160	188, 237
Heptachlor	22.19	272	274, 270
Methyl parathion	22.51	263	109, 125
d_{10}-Chlorpyriphos	23.30	324	107, 209
Chlorpyriphos	23.48	314	199, 197
Fenthion	24.00	278	125, 109
Ethyl parathion	24.05	291	109, 97
Heptachlor epoxide	25.15	353	355, 81
Endrin	27.55	263	265, 261
Endosulfan sulphate	30.60	272	274, 387
Endrin ketone	32.40	317	315, 319

[285138-81-0] was purchased from Cambridge Isotopes (Andover, MA). All chemicals used were of reagent quality.

Anhydrous citric acid was purchased from Riedel de Haën (Seelze, Germany); saccharose was from Fluka (Buchs, Switzerland), pectin was from Sigma Aldrich (St. Louis, MO, USA), acetone and methanol were from Merck (Darmstadt, Germany).

A Milli-Q Plus ultrapure water system from Millipore (Milford, MA) was always used.

2.2. Preparation of the working solutions

2.2.1. Standard solutions

Intermediate standard working solutions were prepared monthly by diluting 1:50 the stock solutions with acetone. The IS intermediate working solution was prepared by diluting 1:20 with acetone. The intermediate standard solutions were diluted to 0.2 ng/μL for any analyte with the exception of alachlor (0.47 ng/μL), chlorpyriphos methyl (0.23 ng/μL) and the IS d_{10}-chlorpyriphos (0.5 ng/μL), to draw the extraction time profile curves, to perform the recovery tests and to construct the calibration curves. The different concentrations of some analytes in the intermediate standard solutions are due to the different origin of the commercially available stock solutions. The analyte solutions, except the IS one, were further diluted 1:10 for the obtainment of the first two calibration points. These solutions were prepared weekly. All solutions were stored in the dark at −4 °C.

2.2.2. Matrix solutions

The synthetic matrices and the commercially available real matrices considered are reported in Table 1.

The pH value of all solutions was about 2.5.

2.3. Sample preparation

2.3.1. Extraction time profiles

The extraction time profiles for any analyte were obtained mixing aliquots of solutions as shown in Table 2. All these solutions were spiked with 1.5 ng of IS, 2.35 ng of alachlor, 1.15 ng of chlorpyriphos methyl and 1 ng for the other pesticides.

2.3.2. Effect of methanol addition

To find the best analytical conditions for the extraction of the pesticides of different polarity, 5 mL of matr.A were diluted either with 5 mL of water or with 5 mL of water added with 1 mL, 2 mL, 3 mL of methanol, respectively. Each of these four solutions was spiked with 1.5 ng of IS, 2.35 ng of alachlor, 1.15 ng of chlorpyriphos methyl and 1 ng for the other pesticides.

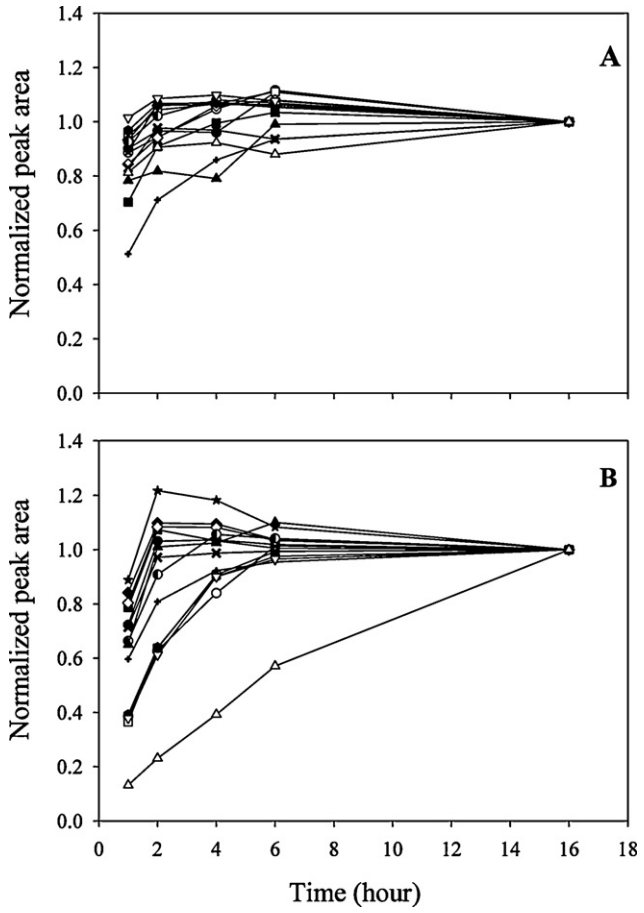

Fig. 1. SBSE desorption time profile, in terms of ratios between the peak areas at defined times and the peak area after 16 h of equilibration, for the studied pesticides in 9 mL of water and 1 mL of methanol (A) and 5 mL of water, 4 mL of matr.A and 1 mL of methanol (B). The matrices were spiked with 1.5 ng of IS, 2.35 ng of alachlor, 1.15 ng of chlorpyriphos methyl and 1 ng for the other pesticides. (○) d_{10}-chlorpyriphos; (●) chlorpyriphos methyl; (■) methyl parathion; (□) chlorpyriphos; (♦) fenthion; (◊) ethyl parathion; (⬢) heptachlor epoxide; (◐) endosulfan sulphate; (⊓) endrin ketone; (⊓) lindane; (+) alachlor; (▲) terbuphos; (▽) endrin; (△) heptachlor.

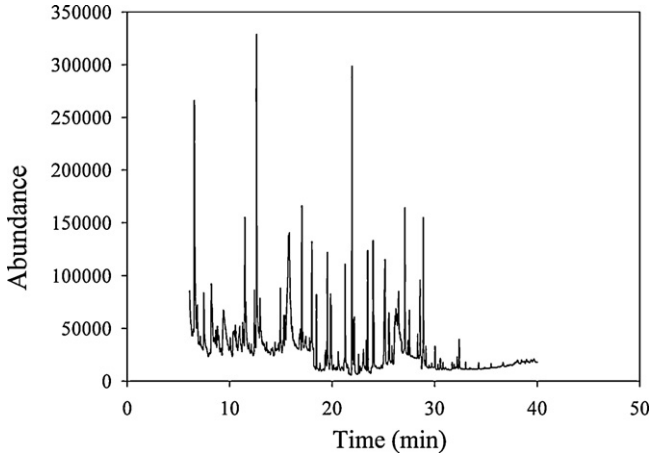

Fig. 2. GC–MS chromatogram obtained recording the total ion current in a aqueous methanolic solution spiked with 0.4 ng mL^{-1} of each pesticide studied except for alachlor, 0.94 ng mL^{-1}, and chlorpyriphos methyl, 0.46 ng mL^{-1}. Operative conditions as in Table 3.

Table 5
Effect of the methanol addition (1:10) on the recovery of pesticides in spiked water (rec%$_w$), in the spiked real matrix A (rec%). The last column reports the apolarity rank of the pesticides studied in terms of the octanol–water distribution coefficients $K_{o/w}$.

Analyte	Rec%$_w$		Rec%		log $K_{o/w}$
	No methanol	Methanol	No methanol	Methanol	
Heptachlor	100.0	49.0	17.5	38.5	6.10
Endrin ketone	95.9	70.7	85.8	106.1	5.33
Endrin	100.0	91.5	59.6	81.7	5.20
Heptachlor epoxide	98.5	65.2	62.4	79.7	4.98
Chlorpyriphos	95.0	58.2	82.9	107.3	4.96
d_{10}-Chlorpyriphos	99.0	63.5	81.8	96.1	4.96
Terbuphos	97.9	22.8	66.7	88.2	4.48
Chlorpyriphos methyl	97.9	62.9	103.8	113.8	4.31
Fenthion	96.5	65.0	99.9	110.0	4.09
Ethyl parathion	96.3	54.8	103.6	110.7	3.83
Lindane	90.5	19.6	72.7	87.9	3.72
Endosulfan sulphate	96.3	68.2	116.0	123.4	3.66
Alachlor	75.6	39.0	86.6	93.0	3.52
Methyl parathion	80.7	32.8	116.0	120.4	2.86

2.3.3. Recovery

The limiting yield of recovery for each analyte from water solution (rec%$_w$) in a single extraction was evaluated performing three subsequent equilibration steps with the same bar on the same solution made up of 10 mL of water, 1 mL of methanol, 1.5 ng of IS, 2.35 ng of alachlor, 1.15 ng of chlorpyriphos methyl and 1 ng for the other pesticides. The peak areas A'_{1w}, A'_{2w}, A'_{3w} of every analyte after the three subsequent equilibration steps were recorded. The overall experiment was replicated obtaining A''_{1w}, A''_{2w}, A''_{3w}. The yield was calculated as:

$$\text{rec\%}_w = \frac{A'_{1w} + A''_{1w}}{(A'_{1w} + A'_{2w} + A'_{3w}) + (A''_{1w} + A''_{2w} + A''_{3w})} \times 100$$

The yield of recovery for each analyte from a real matrix (rec%), made up of 5 mL of matr.A, 5 mL of water,1 mL of methanol, and spiked as above reported, was obtained as:

$$\text{rec\%} = \left(\frac{\bar{A}_1}{\bar{A}_{1w}}\right) \times 100$$

where $\bar{A}_1$ and $\bar{A}_{1w}$ are means of seven peak area values obtained from the first equilibration step in real matrix and in water, respectively.

2.3.4. Calibration solutions

Calibration curves were constructed with the following six solutions: 5 mL of water, 1 mL of methanol plus (1) 5 mL of matr.A; (2) 5 mL of matr.B; (3) 5 mL of matr.C; (4) 1 g of matr.D and 4 mL of water; (5) 5 mL of matr.4; (6) 5 mL of water. Each solution was added at different pesticide levels using suitable aliquots of standard solutions.

2.3.5. Instrumentation and operating conditions

The sampling apparatus was a stir bar (Twister, Gerstel, Muellheim, a/d Ruhr, Germany) 10 mm long, coated with 1.0 mm polydimethylsiloxane (PDMS) layer (63 μL). In all the sorption experiments the rotation speed was 1400 rpm and the temperature was 30 °C. The injection apparatus from Gerstel was made up of the following modules from Gerstel: a multipurpose sampler (MPS), a thermal-desorption unit (TDU), a cooled injection system (CIS) and a programmed temperature vaporization injector (PTV). This unit was placed on an Agilent 6890 GC (Agilent Technologies, Little Falls, DE) connected to an Agilent 5975 quadrupole mass spectrometer. GC analyses were performed on a 30 m × 0.25 mm i.d., 0.25 μm film thickness VF-Xms column (Varian Inc., Lake Forest, CA). Helium was the carrier gas. Blank runs of the stir bar were carried out before and after each analysis to verify the absence of any carry-over effect.

The optimized operating conditions for thermal desorption and GC run are summarized in Table 3. The optimization procedure followed was the single-factor-at-a-time strategy. The transfer line and the electron ionization (EI) source temperatures were 200 °C and 150 °C, respectively. The electron energy was 70 eV. All the analyses were carried out in single ion monitoring (SIM) mode. Table 4 reports the retention times and the m/z values of the ions used for the quantitation and confirmation of the target analytes.

2.4. Statistical analysis

The Cochran test was used to check the heteroscedasticity of the experimental measurements at a fixed matrix and various calibration concentrations and the homoscedasticity of the data set measured at a fixed concentration varying the matrix [13]. The Shapiro–Wilk test [14] and the Grubbs test [15] were used for establishing the normality and the absence of outliers, respectively, for the data sets obtained at a fixed concentration varying the matrices in the calibration procedure. The Grubbs test on the intercepts and on the slopes of the calibration curves for the single matrices was used to examine the presence of outlying curves. The 5% significance level was used for all tests.

2.4.1. Matrix-specific and matrix-comprehensive calibration functions

The calibration straight line relevant to the jth matrix, $\hat{a}_j + \hat{b}_j x$, $j = 1, 2, \ldots, J$, was calculated using I data points and exploiting the weighted regression because of the non-constancy of the measurement variances with the concentration level. The inverse of the experimental variance $s_j^2(x)$ of the replicate responses at each concentration x was adopted as the weighting factor $w_j(x)$ in the weighted regression. Then an averaged overall calibration straight line $\hat{a} + \hat{b}x$, where $\hat{a} = (1/J)\sum_{j=1}^{J} \hat{a}_j$ and $\hat{b} = (1/J)\sum_{j=1}^{J} \hat{b}_j$, was calculated to account for matrix-induced deviations together with an averaged $(1-\alpha)100\%$ prediction interval for measurement values at each x [6]:

$$\hat{a} + \hat{b}x \pm t_{1-\alpha/2,\nu} \left\{ \frac{s^2(x) + \hat{\text{var}}(\text{estimation error})}{J} \right\}^{1/2} \quad (1a)$$

where $\nu = J(I-2)$, $s^2(x) = (1/J)\sum_{j=1}^{J} s_j^2(x)$,

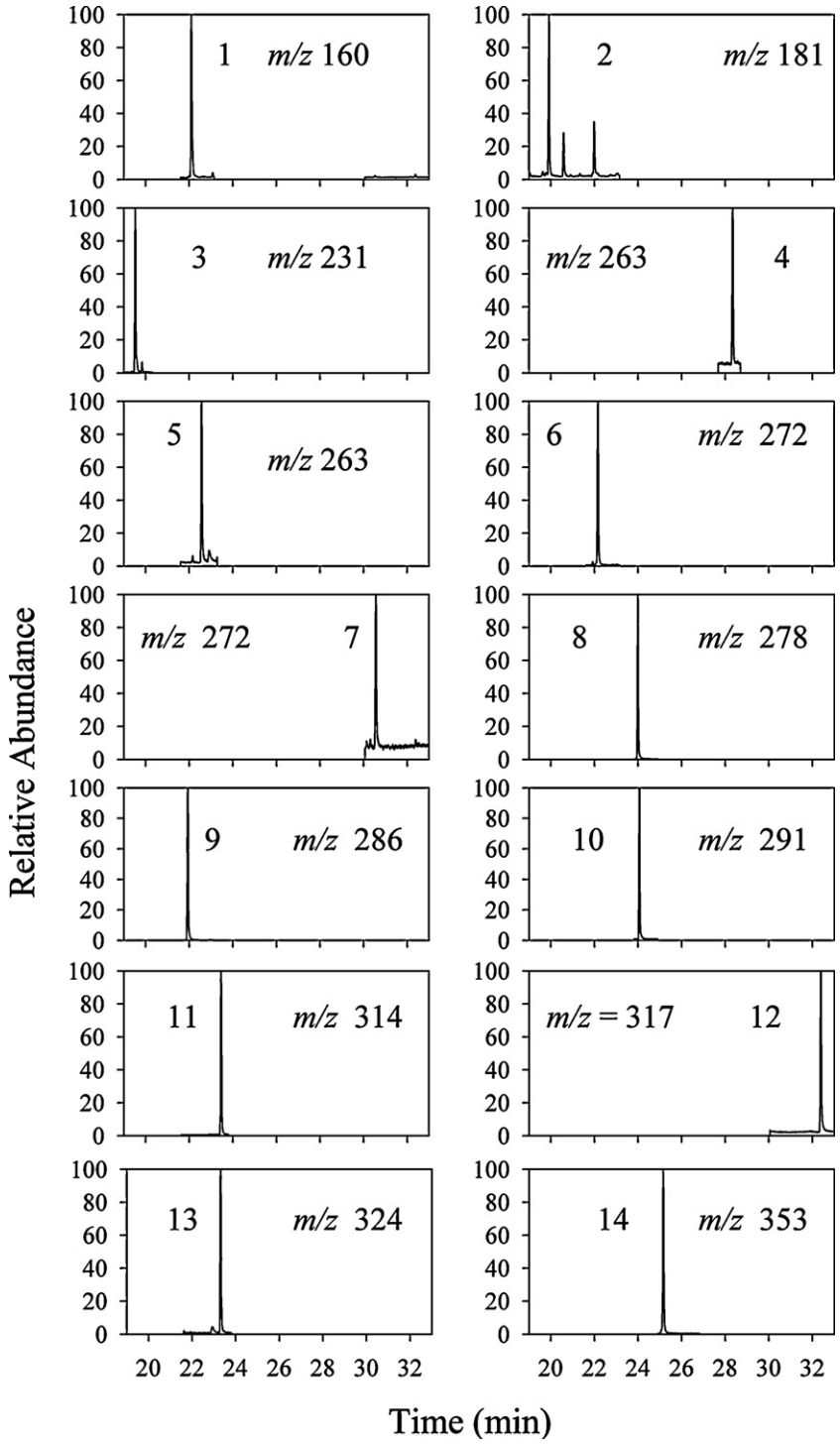

Fig. 3. GC–MS chromatogram obtained in SIM mode of a standard solution with the following concentration level: 0.4 ng mL^{-1} of each pesticide studied except for alachlor, 0.94 ng mL^{-1}, and chlorpyriphos methyl, 0.46 ng mL^{-1}. Peak assignments: 1, alachlor; 2, lindane; 3, terbuphos; 4, methyl parathion; 5, endrin; 6, heptachlor; 7, endosulfan sulphate; 8, fenthion; 9, chlorpyriphos methyl; 10, ethyl parathion; 11, chlorpyriphos; 12, endrin ketone; 13, d_{10}-chlorpyriphos; 14, heptachlor epoxide.

vâr(estimation error)

$$= \left(\frac{1}{J}\right) \sum_{j=1}^{J} \left\{ \left(s^2_{y/x}\right)_j \left(\frac{1}{\sum_{i=1}^{I} w_j(x_i)} + \frac{(x-\bar{x}_j)^2}{\sum_{i=1}^{I} w_j(x_i)(x_i-\bar{x}_j)^2} \right) \right\} \quad (1b)$$

$\left(s^2_{y/x}\right)_j = \sum_{i=1}^{I} w_j(x_i)(y_j(x_i) - \hat{y}_j(x_i))^2/(I-2)$ is the jth weighted residual variance, $y_j(x_i)$ and $\hat{y}_j(x_i) = \hat{a}_j + \hat{b}_j x_i$ are the experimental and the weighted predicted value at x_i for the jth calibration run, respectively, and $\bar{x}_j = \sum_{i=1}^{I} w_j(x_i)x_i / \sum_{i=1}^{I} w_j(x_i)$ (see Tables 1 and 2 in Ref. [10]). Eq. (1a) reflects the assumption of the equivalence between data set and matrix-specified calibration straight line set. Therefore, it is obtained from the theory regarding the calculation of the $(1-\alpha)100\%$ prediction interval for a single value Y starting from the mean, in the present case from the overall calibration line, $(Y - (\hat{a} + \hat{b}x))/s_{Y-(\hat{a}+\hat{b}x)} = t$ [16].

The variance $s^2(x) = (1/J)\sum_{j=1}^{J} s_j^2(x)$, calculated as the pooled variance of the experimental and statistically equal variances $s_j^2(x)$,

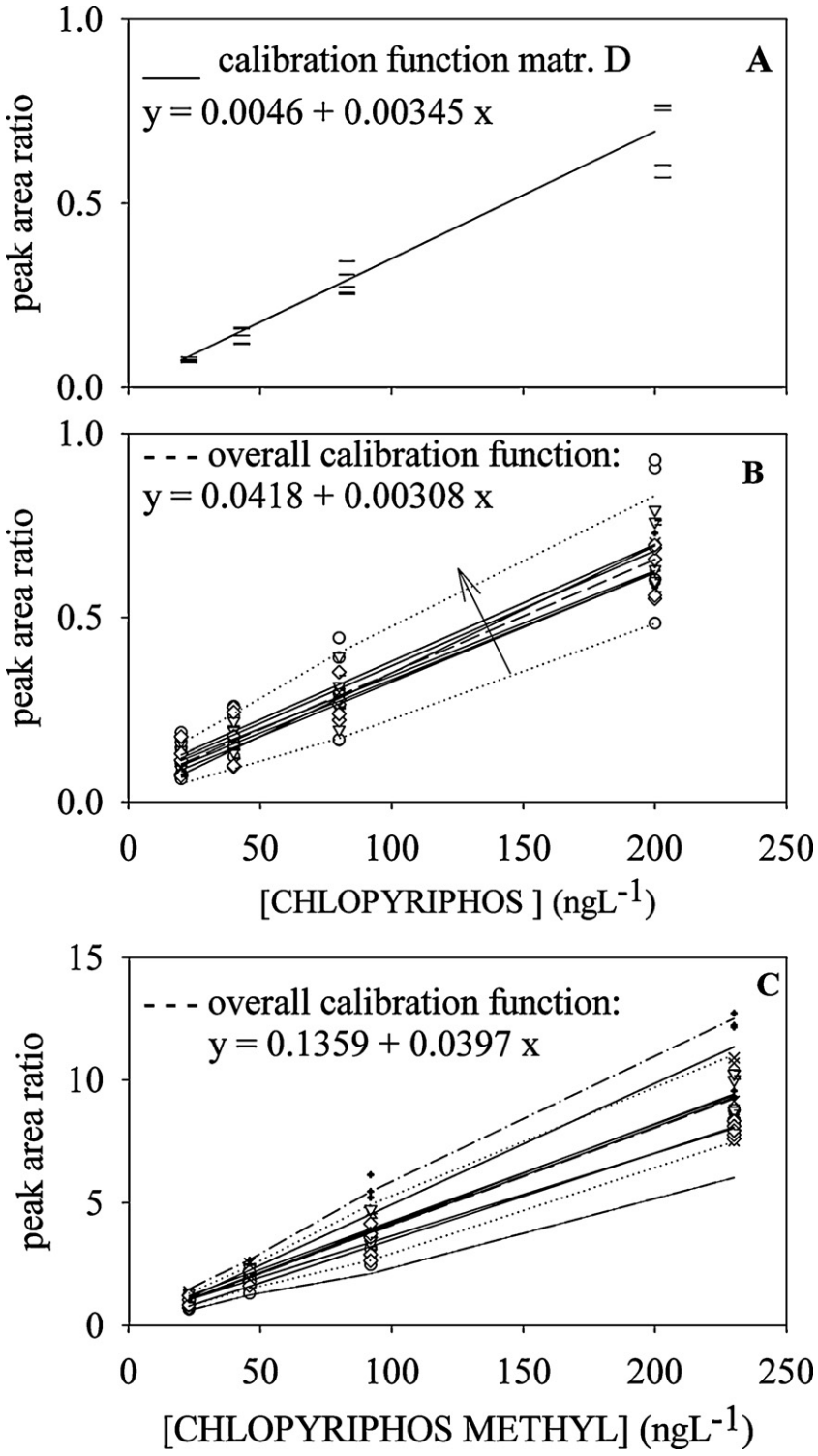

Fig. 4. Weighted calibration curve of chlorpyriphos when five replicate analyses were done in spiked matr.D (A). The experimental data are ratios between the peak areas of the analyte and those of d_{10}-chlorpyriphos. Plots of the ratios of the peak areas of chlorpyriphos (B) and chlorpyriphos methyl (C) with the d_{10}-chlorpyriphos internal standard versus the analyte concentration levels of the standard solutions. matr.A (+), matr.4 (□), matr.B (o), water (▽), matr.C (◊), matr.D (−). The continuous lines are the calibration functions relevant to each matrix obtained via weighted linear regression; the dashed line is the overall calibration function; the dotted lines are the 90% prediction intervals calculated by means of Eq. (1a). The dash-dotted lines in (C) are 90% prediction intervals calculated by Eq. (2).

$j = 1, 2, \ldots, J$, furnishes, as usual, an estimate of the measurement error $\sigma_0^2(x)$ at fixed x. The right hand side of Eq. (1b) is a mean of the estimates at x of the uncertainties of the matrix-specified calibration functions.

The effective presence of matrix-induced deviations was checked by a significance test, using the statistic $(p-\alpha)/\sqrt{\alpha(1-\alpha)/I \cdot J}$, where p is the proportion of experimental data outside the $(1-\alpha)100\%$ prediction interval given by Eq. (1a). This statistic asymptotically coincides with the normal standardized variate Z [17].

When the experimental proportion p appears significantly larger than α, the simple model underlying Eq. (1a) does not hold,

Table 6
Detection limits x_D (ng L^{-1}) and confidence interval limits x^- (ng L^{-1}), x^+ (ng L^{-1}) for the discriminated concentration value $x = 80$ ng L^{-1} obtained from the calibration curves relevant to two real matrices and from the overall function. The first two columns show values obtained for the matrices whose calibration curves had the larger and the lower slope, respectively. The detection limits and the confidence limits were calculated from 90% two-sided prediction intervals ($\alpha = \beta = 0.05$).

	Chlorpyriphos		
	Matr.D	Matr.C	Overall
x_D	10	68	43
x^-, x^+	58, 121	47,128	51,126
	Chlorpyriphos methyl		
	Matr.A	Matr.C	Overall
x_D	7	34	21
x^-, x^+	59, 126	61,103	56,135
	Lindane		
	Matr.D	Matr.B	Overall
x_D	24	36	39
x^-, x^+	61, 110	60,109	47,182

namely the different calibration curves cannot be considered as repeated observations of the same quantity and the VCM procedure proposed by Juelicher et al. [6] can be adopted.

Following this approach the measurement value $y_j(x)$ at concentration level x for the jth matrix is again assumed to be a random variable normally distributed with expectation value equal to $a + bx$ but with variance $\sigma^2_{yj(x)} = \sigma^2_0(x) + \mathrm{var}(a_j + b_j x)$, where $\mathrm{var}(a_j + b_j x)$ is an additional component of the variance coming from the matrix-induced error. This means that the matrix-induced deviation is a random variable with zero mean.

The $(1-\alpha)100\%$ prediction interval at x with the addition of the matrix-induced error is modified into:

$$\hat{a} + \hat{b}x \pm t_{1-\alpha/2,\nu} \left\{ s^2(x) + \hat{\mathrm{var}}(\text{estimation error}) + \hat{\mathrm{var}}(a_j + b_j x) \right\}^{1/2} \quad (2)$$

where $\nu = J - 1$, and $\hat{\mathrm{var}}(a_j + b_j x)$ is an estimate of $\mathrm{var}(a_j + b_j x)$.

The term $\hat{\mathrm{var}}(a_j + b_j x)$ estimates how the matrix calibration curves scatter around the overall calibration curve and is calculated as [6]:

$$\hat{\mathrm{var}}(a_j + b_j x) = s^2_{\hat{a}_j + \hat{b}_j x} - \hat{\mathrm{var}}(\text{estimation error}) \quad (3a)$$

when the difference on the right hand side of Eq. (3a) is positive, or as:

$$\hat{\mathrm{var}}(a_j + b_j x) \quad (3b)$$

when the difference is negative. The difference $s^2_{\hat{a}_j + \hat{b}_j x} - \hat{\mathrm{var}}$(estimation error) results to be positive when the matrix-induced deviations are effective, is theoretically zero in the absence of these deviations, and can appear negative for the presence of experimental uncertainty.

In Eq. (3a) the term $s^2_{\hat{a}_j + \hat{b}_j x} = 1/(J-1)\sum_{j=1}^{J} [\hat{a}_j + \hat{b}_j x - (\hat{a} + \hat{b}x)]^2$ is the empirical variance of the estimated responses $\hat{a}_j + \hat{b}_j x$ at concentration level x [6].

2.4.2. Detection limit and inverse-predicted concentration uncertainty

The detection limit was calculated with the Hubaux–Vos approach both employing the matrix-specified calibration curve and the overall one [18]. This procedure requires the calculation of the relevant prediction bands taking into account the uncertainty of the measurements and of the calibration straight line. Therefore, for the jth matrix-specified calibration curve the limits of the weighted $(1-\alpha)100\%$ prediction band were calculated by means of the equation:

$$\hat{a}_j + \hat{b}_j x_i \pm t_{1-\alpha/2,\nu} \left[s^2_j(x_i) + (s^2_{y/x})_j \left(\frac{1}{\sum_{i=1}^{I} w_j(x_i)} + \frac{(x_i - \bar{x}_j)^2}{\sum_{i=1}^{I} w_j(x_i)(x_i - \bar{x}_j)^2} \right) \right]^{1/2}$$

where $\nu = I - 2$. When the overall calibration line $\hat{a} + \hat{b}x$ is used, two different situations can occur, i.e. absence or presence of matrix-induced deviations. In the former case the detection limit is calculated using the prediction band given by Eq. (1a), in the latter one using Eq. (2). Whatever be the prediction band used, the underlying concept is the same:

(i) the critical level L_C is defined in the signal domain as the level exceeded at $x = 0$ with probability α. In the particular case of the VCM approach the critical level L_C is given by:

$$\frac{L_C - \hat{a}}{(s^2(x=0) + \hat{\mathrm{var}}(a_j + b_j x)_{x=0} + \hat{\mathrm{var}}(\hat{a}))^{1/2}} = t_{1-\alpha,J-1}$$

where $s^2(x=0)$ was chosen equal to the measurement variance value at the first concentration level of calibration design for the analyte at hand and the last term is given by (see Eq. E33 in Ref. [7]):

$$\hat{\mathrm{var}}(\hat{a}) = \frac{1}{J}\hat{\mathrm{var}}(a_j + b_j x)_{x=0} + \frac{\hat{\mathrm{var}}(\text{estimation error})}{J}$$

(ii) the detection limit x_D in the concentration domain, i.e. the concentration which generates a signal lying under L_C with probability β, is the abscissa of the intersection of the parallel line to the x axis passing through L_C with the lower one sided $(1-\beta)100\%$ prediction function. Alternatively, x_D is determined graphically putting equal to $1-\beta$ the power function $p(x)$ defined by the equation:

$$p(x) = 1 - F_{J-1,\delta_x} \left(t_{1-\alpha,J-1} \left(\frac{s^2(x) + \hat{\mathrm{var}}(a_j + b_j x)_{x=0} + \hat{\mathrm{var}}(\hat{a})}{s^2(x) + \hat{\mathrm{var}}(a_j + b_j x) + \hat{\mathrm{var}}(\hat{a})} \right)^{1/2} \right)$$

where F_{J-1,δ_x} is the distribution function of the non-central t-distribution with $J-1$ degrees of freedom and non-centrality parameter $\delta_x = \hat{b}x/(s^2(x) + \hat{\mathrm{var}}(a_j + b_j x) + \hat{\mathrm{var}}(\hat{a}))^{1/2}$ (see Eqs. E36 and E37 in Ref. [7]).

The $(1-\alpha)100\%$ confidence interval limits x_0^- and x_0^+ of the inverse-predicted concentration x_0 corresponding to the response y_0, are obtained graphically by intersecting the appropriate $(1-\alpha)100\%$ two sided prediction band with the straight line $y = y_0$ [19,20].

3. Results and discussion

3.1. Recovery

3.1.1. Extraction-time profile

The dependence of the extraction of the bar from the solutions was evaluated measuring the peak areas of the different analytes at various equilibration times. The trends of the recovered quantities for the spiked aqueous-methanol solution (10:1, v/v) and for the real matrix A, diluted with water and methanol (5:5:1, v/v/v), are shown in Fig. 1a and b, respectively. It is apparent that only heptachlor shows an anomalous behaviour in real matrix. A similar behaviour is shown by the different analytes in the different matrices, with the common trend that the presence of pectin in the synthetic matrices and of fruit pulp in the real matrices decreases the recovery efficiency. An extraction period of 6 h was selected as a good compromise between yield and practicality.

3.1.2. Effect of methanol addition

As described in the literature the adsorption onto the glass walls and the nature of the real matrix influence the recovery of pesticides [2,3]. In fact the extraction of pesticides of different polarity expected on the basis of their octanol–water partition coefficients, $K_{o/w}$, can be more or less modified [21–23]. Addition of methanol, suitable ionic strength, silanization of the glass surface have been suggested as adjustable working parameters. The influence of the methanol content on the amount of the pesticide extracted from the real matr.A is reported in Table 5 (fourth column). The content of methanol (1:10, v/v) appears to favour the extraction of apolar compounds and decrease the extraction of the more polar ones. These results agree with the hypothesis advanced by Sandra et al. [23] who suggest the existence of competitive equilibria between the bar (PDMS phase), the liquid phase and the fruit pulp. The methanol decreases the competitive extraction into the fruit pulp of apolar analytes making them more available for the partition with PDMS. On the basis of these findings calibration curves were done using spiked synthetic matrices containing pectin to simulate the presence of fruit pulp.

3.1.3. Yield of extraction

Table 5 shows the recovery of the different analytes from water and water added with 1 mL of methanol solutions (first and second columns), and from the real matrix A and the real matrix A added with 1 mL of methanol (third and fourth columns). It is apparent that in water a single equilibrium step is practically exhaustive with the third extraction step irrelevant ($A'_3 = A''_3 = 0$). On the basis of this result and of the time profile trend reported above, the yield of recovery from the real matrix A was determined after one equilibration step 6 h long. The data reported in the third column of Table 5 show a large range of recovery values which deserve some comments. The values of the recovery relevant to chlorpyriphos methyl, methyl parathion, chlorpyriphos and endosulfan sulphate are appreciably greater than 100. This fact is explained by the presence of the pesticides in the unspiked matrices, i.e. in the blank solution (data not shown). Therefore these high values are the consequence of endogenous and exogenous compounds. The recovery values larger than 100 for fenthion, ethyl parathion and endrin ketone can be explained as an artefact due to the definition of the recovery for the real matrix in addition to the experimental uncertainty. The artefact arises from the circumstance that the yield $\bar{A}_{1w}$ is about 0.96 and plays the role of denominator. The very low value for heptachlor points out the difficulty of extracting the most apolar compound as a consequence of a significant matrix effect which influences the analyte distribution between solid (lemon pulp) and liquid phases. For this reason the equilibration time is an important parameter for the more apolar pesticides. For the other real matrices and for the solutions added with pectin the influence of methanol follows the trend shown in the fourth column of Table 5.

3.2. Quantitative analysis

Fig. 2 shows, as an example, a chromatogram obtained recording the total ion current in a aqueous methanolic solution spiked with 0.4 ng mL^{-1} of each pesticide studied except for alachlor, 0.94 ng mL^{-1}, and chlorpyriphos methyl, 0.46 ng mL^{-1}.

Fig. 3 shows the chromatographic run obtained recording in SIM mode the current relevant to the target ion chosen for any pesticides considered. To illustrate the features of the experimental data Fig. 4a shows the peak area ratios between peak areas of chlorpyriphos and peak areas of the IS at four concentration levels and the weighted calibration curve in the real matr.D, i.e. in a mixed fruit-based juice. At each calibration level five replicates were done performing the entire analytical procedure from the extraction step to the GC–MS analysis. In this way the contribute of the time-induced deviations is introduced in the variability of the replicates.

The non-constancy of the measurement variances with the concentration levels was established via Cochran test. The inverses of the experimental variances were the weighting factors in the weighted regression. Fig. 4b shows the experimental peak area ratios for chlorpyriphos and the IS in the real matrices A–D, in water, and in the synthetic matrix indicated as matr.4 together with the relevant weighted calibration curves. A slight contribute to the variance of the measures at each concentration level, that is to the heteroscedasticity, coming from the use of different matrices, is evident even if an isotopically labelled internal standard is used. A higher dispersion of the experimental data at each concentration level is found varying the matrix when the behaviour of chlorpyriphos methyl is examined in the absence of its proper isotopically labelled IS, as shown in Fig. 4c. Analogous behaviours are shown by the other analytes considered for which labelled ISs were not available.

Fig. 4a–c shows that the dispersion of the experimental data is due to different causes: instrumental uncertainty and handling of the solutions (Fig. 4a), change of the matrix, whose effect is differently corrected by the use of labelled (Fig. 4b) or unlabelled (Fig. 4c) IS. However, a closeness of the calibration curves relevant to various matrices is apparent in both instances.

In routine analysis of pesticides in several matrices the analytical procedures to be adopted must offer the best compromise between costs and benefits. The closeness of the calibration curves in Fig. 4b and c suggests to verify whether they can be properly substituted for by overall calibration straight lines with intercepts and slopes given by the means of the corresponding parameters pertinent to each matrix. The Grubbs test on the intercepts and on the slopes confirms the closeness of the calibration functions for each analyte varying the matrix so indicating the absence of outlying calibration curves. This result pointed out that significant matrix effects were corrected in the concentration range explored even using unlabelled ISs [6]. Consequently an overall calibration function was constructed for any pesticide. To properly utilize the overall calibration function in quantitative analysis its prediction band must be calculated. Actually the uncertainty of the discriminated concentration value depends on the width of the prediction band. Fig. 4b shows that the 90% prediction interval calculated by Eq. (1a) covers the experimental distribution of the measurements

for chlorpyriphos, whereas Fig. 4c shows that even the 98% prediction interval includes less than 98% of the measurement values for chlorpyriphos methyl. This latter observation points out the presence of residual matrix- and time-induced deviations.

The highlighted inadequacy of the prediction interval calculated by Eq. (1a), when the unlabelled internal standard was used, required an enlargement of the prediction intervals themselves to account for the greater dispersion of the measurement values. In Fig. 4c, the dashed lines define the 90% prediction interval calculated by Eq. (2), where the VCM theory properly accounts for the residual effects of different matrices when the single calibration functions are substituted for by an overall one. However, the enlargement of the prediction interval implies a wider uncertainty in discriminated concentration values and an increment of the detection limit values.

To evaluate the effectiveness of coupling SBSE/TD/GC–MS and VCM method, the detection limits and uncertainty intervals of discriminated concentrations of three pesticides were determined in two real matrices from matrix-specified calibration curves, and their values were compared with those obtained using the overall calibration function. Table 6 shows the results obtained for three pesticides which are particularly representative of the set of pesticides studied. The analytes chosen were chlorpyriphos, since its isotopically labelled IS was used in all experiments, methyl chlorpyriphos and lindane as quite similar or quite different pesticide from the IS used. Further for the selected pesticides the matrix-specified calibration curves were chosen on the basis of their greatest distance from the corresponding overall curves. From the results shown in Table 6 it appears that the use of an overall function is equivalent to the employment of matrix-specified function for chlorpyriphos for which the isotopically labelled IS is used. In the absence of the most appropriate IS the use of the overall functions appears satisfactory for routine analyses.

4. Conclusions

The combination of the SBSE–TD–GC–MS technique and the VCM statistical procedure is an effective strategy to decrease times and costs of the adopted analytical method when several matrices must be analyzed and a overall calibration curve is tentatively used in the context of pesticides analysis in fruit-based soft drinks. The VCM approach furnishes an overall calibration function with its appropriate prediction band. It allows the calculation, via the application of the Hubaux–Vos method, of an inter-matrix detection limit and of an inter-matrix confidence interval of a discriminated concentration value.

The enlargement of these typical parameters, due to the matrix- and time-induced deviations, is a drawback which is largely overcome by the benefits in time and cost mainly in routine analysis.

Acknowledgement

The financial support of the Italian Ministry for Universities and Research (MIUR) is gratefully acknowledged.

References

[1] F. David, B. Tienpont, P. Sandra, LC–GC Eur. 16 (2003) 410.
[2] V.M. León, B. Alvarez, M.A. Cobollo, S. Muñoz, I. Valor, J. Chromatogr. A 999 (2003) 1.
[3] P. Sandra, B. Tienpont, F. David, J. Chromatogr. A 1000 (2003) 299.
[4] C. Blasco, M. Fernández, Y. Picó, G. Font, J. Chromatogr. A 1030 (2004) 77.
[5] C. Bicchi, C. Cordero, P. Rubiolo, P. Sandra, Eur. Food Res. Technol. 216 (2003) 449.
[6] B. Juelicher, P. Gowik, S. Uhlig, Analyst 123 (1998) 173.
[7] B. Juelicher, P. Gowik, S. Uhlig, Analyst 124 (1999) 537.
[8] I. Lavagnini, B. Fedrizzi, G. Versini, F. Magno, Rapid Commun. Mass Spectrom. 23 (2009) 1167.
[9] S.R. Searle, G. Casella, C.E. McCulloch, Variance Components, Wiley, New York, 1992.
[10] L. Brueggemann, P. Morgenstern, R. Wennrich, Accredit. Qual. Assur. 10 (2005) 344.
[11] Y. Picó, C. Blasco, G. Font, Mass Spectrom. Rev. 23 (2004) 45.
[12] J.F. García-Reyes, B. Gilbert-López, A. Molina-Díaz, A.R. Fernández-Alba, Anal. Chem. 80 (2008) 8966.
[13] A. Cohen, J.I. Marden, Ann. Stat. 17 (1989) 236.
[14] S.S. Shapiro, M.B. Wilk, Biometrika 52 (1965) 591.
[15] F. Grubbs, Technometrics 11 (1969) 1.
[16] K.A. Brownlee, Statistical Theory and Methodology in Science and Engineering, Wiley, New York, 1960.
[17] W.J. Dixon, F.J. Massey, Introduction to Statistical Analysis, McGraw-Hill, New York, 1957.
[18] A. Hubaux, G. Vos, Anal. Chem. 4 (1970) 849.
[19] R.G. Miller, Simultaneous Statistical Inference, McGraw-Hill, New York, 1966.
[20] I. Lavagnini, F. Magno, Mass Spectrom. Rev. 26 (2007) 1.
[21] P. Sandra, B. Tienpont, J. Vercammen, A. Tredoux, T. Sandra, F. David, J. Chromatogr. A 928 (2001) 117.
[22] C. Bicchi, C. Cordero, C. Iori, P. Rubiolo, P. Sandra, J.H. Yariwake, V.G. Zuin, J. Agric. Food Chem. 51 (2003) 27.
[23] P. Sandra, B. Tienpont, F. David, RIC-an-2003-1 at www.gerstelus.com.